



# Systematic variation of bedrock channel gradients in the central Oregon Coast Range: implications for rock uplift and shallow landsliding

Jeremiah S. Kobor\*, Joshua J. Roering

*Department of Geological Sciences, University of Oregon, Eugene, OR 97403, USA*

Received 24 October 2003; received in revised form 18 February 2004; accepted 19 February 2004

Available online 10 May 2004

## Abstract

In tectonically active regions, bedrock channels play a critical role in dictating the pace of landscape evolution. Models of fluvial incision into bedrock provide a means of investigating relationships between gradients of bedrock channels and patterns of active deformation. Variations in lithology, orographic precipitation, sediment supply, and erosional processes serve to complicate tectonic inferences derived from morphologic data, yet most tectonically active landscapes are characterized by these complexities. In contrast, the central Oregon Coast Range (OCR), which is situated above the Cascadia subduction zone, has experienced rock uplift for several million years, did not experience Pleistocene glaciation, boasts a relatively uniform lithology, and exhibits minor variations in precipitation. Although numerous process-based geomorphic studies suggest that rates of erosion across the OCR are relatively constant, it has not been demonstrated that bedrock channel gradients in the region exhibit spatially consistent values. Analysis of broadly distributed, small drainage basins ( $\sim 5$ – $20$  km) in the central OCR enables us to explore regional variability in bedrock channel gradients resulting from differential rock uplift or other sources. Consistent with previous studies that have documented local structural control of deformed fluvial terraces in the western portion of our study area, our data reveal a roughly 20-km-wide band of systematically elevated channel slopes (roughly twice the background value), roughly coincident with the strike of N–S-trending mapped folds. Although many factors could feasibly generate this pattern, including variable rock strength, precipitation gradients, or temporal or spatial variations in forearc deformation, the elevated bedrock channel slopes likely reflect differential rock uplift related to activity of local structures. Importantly, our analysis suggests that rock uplift and erosion rates may vary systematically across the OCR. Although our calculations were focused on the fluvial-dominated portion of study basins, our results have implications for upstream areas, including unchanneled valleys that often serve as source areas for long-runout debris flows. Zero-order basins (or topographic hollows) within the N–S-trending band of elevated channel slopes tend to be steeper than adjacent areas and may experience more frequent evacuation by shallow landsliding. Thus, this region of the OCR may be highly sensitive to land use practices and high-intensity rainstorms.

© 2004 Elsevier B.V. All rights reserved.

*Keywords:* Oregon Coast Range; Stream power; Differential uplift; Fluvial incision; Shallow landslide

\* Corresponding author. Department of Geology, Northern Arizona University, Flagstaff, AZ 86011, USA. Tel.: +1-928-213-5472.

*E-mail address:* [jsk23@dana.ucc.nau.edu](mailto:jsk23@dana.ucc.nau.edu) (J.S. Kobor).

## 1. Introduction

One goal of the recently emergent field of tectonic geomorphology is to characterize relationships be-

tween tectonic deformation and surficial forms and processes. Of principle interest is the ability to explore rates and patterns of active deformation directly from landscape topography (e.g., Ahnert, 1970; Ohmori, 1993; Granger et al., 1996; Hurtrez and Lucazeau, 1999; Kirby and Whipple, 2001; Finlayson et al., 2002; Montgomery and Brandon, 2002; Kirby et al., 2003). The development of geomorphic transport laws is critical, enabling quantification of the linkage between process and form (Dietrich et al., 2003). Well-tested theories are necessary to derive tectonic insights from morphology; however, geomorphic models for different processes are in various stages of development.

In actively uplifting regions, bedrock channel networks transmit the signal of rock uplift, such that fluvial incision ultimately controls landscape denudation by limiting the relief structure of drainage basins and dictating boundary conditions for hillslope processes (e.g., Whipple and Tucker, 1999). The ubiquitous nature of bedrock channels in tectonically active landscapes has led to numerous studies of their dynamics (e.g., Seidl and Dietrich, 1992; Howard et al., 1994; Hancock et al., 1998; Whipple and Tucker, 1999; Snyder et al., 2000; Whipple et al., 2000; Kirby et al., 2003; van der Beek and Bishop, 2003). Furthermore, it has been demonstrated that analysis of bedrock channel incision provides a powerful tool to explore rates and patterns of active deformation (e.g., Kirby and Whipple, 2001).

Among physically based models of bedrock channel incision, the stream power (or shear stress) incision model has been most widely applied towards assessing the balance between rock uplift and channel incision in active tectonic areas (Snyder et al., 2000; Kirby and Whipple, 2001; Kirby et al., 2003). The stream power model is built on the notion that the rate of bedrock channel incision ( $E$ ) is a power law function of unit stream power or basal shear stress. Using hydraulic relations, the stream power law can be cast in terms of drainage area ( $A$ ) and local channel slope ( $S$ ) (Howard and Kerby, 1983):

$$E = KA^m S^n \quad (1)$$

where  $K$  is the erosion coefficient, and  $m$  and  $n$  are empirically derived constants whose values have been

estimated in several landscapes (see Snyder et al., 2000, for full derivation).

Numerous studies have applied the model to field and topographic data (e.g., Howard and Kerby, 1983; Seidl and Dietrich, 1992; Sklar and Dietrich, 1998; Stock and Montgomery, 1999; Snyder et al., 2000), and estimates for the values of  $K$  and  $n$  vary widely. Stock and Montgomery (1999) found at least two end-member incision laws and suggested that  $K$  varied over five orders of magnitude, depending on lithology and climate.  $K$  has also been shown to vary with orographic precipitation (Roe et al., 2002), and Snyder et al. (2000) argued for the existence of a feedback loop such that  $K$  varies in concert with uplift rates via changes in orographic precipitation. Sklar and Dietrich (1998) argued that downstream changes in sediment supply may lead to differential bed armoring and availability of scour tools, significantly influencing the value of  $K$  within a basin.

The slope exponent ( $n$ ) is thought to be a function of the dominant erosional process, and Howard and Kerby (1983) showed that incision rates in rapidly eroding badlands were well explained by a stream power model that assumes incision rate is linearly proportional to bed shear stress ( $m \approx 1/3$  and  $n \approx 2/3$ ). Whipple et al. (2000) found that erosion by plucking is consistent with a value of  $n$  between  $\sim 2/3$  and 1 and that erosion by suspended load abrasion is consistent with a value of  $n$  of  $\sim 5/3$ . The  $m/n$  ratio, however, is thought to be independent of the dominant erosion process and from a theoretical standpoint is expected to fall between 0.35 and 0.6 (Whipple and Tucker, 1999). This is consistent with empirical estimates derived from field data (Howard and Kerby, 1983) and with estimates derived from digital topographic data (Whipple and Tucker, 1999; Snyder et al., 2000; Kirby and Whipple, 2001).

Combining the stream power incision model with a statement of conservation of mass yields an expression for the rate of change of channel elevation ( $dz/dt$ ) as given by the balance between uplift rate ( $U$ ) and incision rate (Howard, 1994):

$$dz/dt = U - E = U - KA^m S^n \quad (2)$$

For the case of steady-state landscapes, rock uplift rate is approximately balanced by the rate of denudation and  $dz/dt$  is equal to zero (Whipple and Tucker, 1999;

Snyder et al., 2000). In this scenario, given uniform  $U$  and  $K$  and constants  $m$  and  $n$ , Eq. (2) can be solved for the steady-state channel slope ( $S_{ss}$ ):

$$S_{ss} = (U/K)^{1/n} A^{-m/n} \quad (3)$$

Eq. (3) implies a power law relationship between channel slope and upstream drainage area with channel slope described by

$$S = k_s A^{-\theta} \quad (4)$$

The coefficient,  $k_s$  (often referred to as the steepness index), and the exponent,  $\theta$  (the concavity index), can be measured directly by regression of slope and area data, and data sets approximating this equation have been observed in regions with diverse tectonic settings (e.g., Howard and Kerby, 1983; Seidl and Dietrich, 1992; Stock and Montgomery, 1999; Snyder et al., 2000; Kirby and Whipple, 2001; Kirby et al., 2003). Eqs. (3) and (4) imply the following relationships:

$$\theta = m/n \quad (5)$$

and

$$k_s = (U/K)^{1/n} \quad (6)$$

which are valid only under conditions where the river profile is in steady state with respect to current tectonic and climatic conditions, and both the uplift rate ( $U$ ) and the erosion coefficient ( $K$ ) are constant throughout the channel reach.

It is important to note that a well-constrained power law relationship between drainage area and slope does not necessarily imply the existence of steady-state conditions (Sklar and Dietrich, 1998; Schorghofer and Rothman, 2001). Alternatively, systematic variation of slope–area data may reflect transient response to variable sediment supply, localized debris flow erosion, the frequency of storm events, orographic effects, and variable lithology and incision mechanisms among others. Most generally, values of  $k_s$  and  $\theta$  can vary widely depending on the assemblage of erosional processes. Despite these complexities, as expressed by Dietrich et al. (2003), “uplift undoubtedly steepens rivers and  $k_s$  should vary in response.” Thus, if the process complexities mentioned above can be minimized, Eq. (4) can be a

valuable tool for a reconnaissance-type investigation of spatially variable uplift rates.

In applying Eq. (4) to quantify variations in tectonic forcing, Kirby and Whipple (2001) concluded that the ratio of the exponents on area and slope ( $m/n$ ) was a useful predictor of spatially variable rock uplift rates. Kirby et al. (2003) mapped the distribution of the steepness index along the eastern margin of the Tibetan Plateau and found a zone of anomalously steep channels adjacent to the topographic front, apparently corresponding to a region of high rock uplift. These and other studies have focused on deciphering patterns of tectonic forcing in regions with high rates of deformation (e.g., Snyder et al., 2000; Kirby and Whipple, 2001; Kirby et al., 2003). Such areas tend to be subject to variable lithology and precipitation gradients, which may serve to complicate interpretations of the relationship between bedrock incision and tectonic uplift. While some of these confounding factors have been integrated into Eqs. (1)–(5) in order to explore their influence on system behavior (e.g., Roe et al., 2003), few studies have applied Eq. (1) to landscapes where such complicating factors are minimal or absent (Stock and Montgomery, 1999). Our motivation here is not to provide a rigorous test of slope–area analysis of tectonic forcing, but instead to demonstrate how it may be applied to decipher differential rock uplift in a landscape that is not significantly influenced by glaciation, variable rainfall, or lithologic complexities.

Here, we analyze 111 small ( $\sim 5$ – $20$  km<sup>2</sup>) tributary basins in the central Oregon Coast Range (OCR) to explore relationships between variable rates of rock uplift and bedrock channel slopes. Although some studies have revealed varying rates of Holocene incision and deformed Quaternary fluvial terraces (Personius, 1993, 1995), analyses of sediment production rates (Reneau and Dietrich, 1991; Heimsath et al., 2001) suggest that erosion rates across portions of the OCR are relatively constant over a broad range of spatial and temporal scales. Several studies have used the evidence for erosional equilibrium to calibrate process-based transport models or analyze the efficacy of conceptual models (Roering et al., 1999; Montgomery, 2001), but it has not been demonstrated that channel networks in the OCR exhibit spatially consistent morphology. Local variations in rock uplift may be obscured in coarse region-wide analyses of

channel slopes (Montgomery, 2001). In contrast, systematic analysis of small drainage basins distributed across a landscape may reveal the signature of local tectonic controls allowing direct interpretation of differential rock uplift.

We analyze our OCR data using Eqs. (1)–(5) to address the following questions: (i) Are bedrock channel slopes spatially constant in the OCR and thus consistent with evidence for constant rates of erosion? (ii) Are mapped geologic structures manifested in the morphology of stream channels? And (iii) What are the implications of variable channel gradients for erosional processes (specifically debris flows) that shape mountainous catchments? Our analysis focuses on the fluvial-dominated portion of relatively small basins (much of their upstream area is dominated by debris flow activity as described in Stock and Dietrich, 2003), as their profiles may adjust rapidly to rock uplift and manifest the signature of local tectonic controls.

## 2. Study site: Smith and Siuslaw basins

The OCR is a rugged belt of deeply dissected, elevated topography bounded to the west by the Pacific Ocean and to the east by the Willamette Valley. Structurally, the central OCR is characterized by gentle N- and NE-trending folds (Baldwin, 1956; Wells and Peck, 1961; Snively, 1987; Walker and Duncan, 1989). Bedrock consists primarily of Eocene and Miocene sedimentary rocks with scattered Oligocene intrusives (Wells and Peck, 1961; Walker and Duncan, 1989). We focus on the Smith and Siuslaw basins where lithology is very uniform and the Eocene Tye Formation accounts for ~ 90% of the exposed bedrock (Fig. 1). The Smith Basin drains ~ 900 km<sup>2</sup> of the western OCR and empties into the Umpqua River near Reedsport, OR. The Siuslaw Basin drains ~ 2002 km<sup>2</sup> of the western OCR and empties into the Pacific Ocean near Florence, OR (Fig. 1). These basins were chosen because they are well situated to avoid lithologic complexities and they allow for a range-wide assessment of bedrock channel gradients.

Uplift of the OCR began in the Miocene due to reorganization of the Pacific and Juan de Fuca plates (McNeill et al., 2000). Presently, the Cascadia Subduction Zone lies 60–100 km west of coastal Oregon,

and ongoing subduction continues to drive rock uplift in the OCR. Short-term (~ 40–70 years) uplift rates have been estimated using repeated leveling surveys and tide gauge records. Mitchell et al. (1994) found that present-day uplift rates vary both longitudinally and latitudinally, and identified both NE- and SE-trending axes of uplift. In the region of the OCR studied here, geodetic rates decrease in a north by northeast direction from 3 mm/year south of Reedsport to 1 mm/year north of Florence. Several studies document rock uplift in the last ~ 80–125 ky along coastal Oregon using uplifted marine terraces as a datum (e.g., West and McCrumb, 1988; Kelsey, 1990; Kelsey and Bockheim, 1994; Kelsey et al., 1994, 1996). These terrace uplift rates are generally < 0.4 mm/year, except in locations where late Quaternary faults displace marine benches; systematic variation in long-term rock uplift rates appears to be minimal along our study area's western margin.

Channels are generally free of thick alluvial mantles and are bedrock-dominated due to the mechanically weak nature of the sandstone and the relatively steep channel slopes (Seidl and Dietrich, 1992). Over 100 years of riparian wood removal and accelerated shallow landsliding may have also contributed to the dominance of bedrock (Montgomery et al., 2000). Persistent strath terraces along most OCR channels attest to the long-term requirement of OCR streams to incise bedrock, and evidence of stream capture (Neim, 1976; Baldwin, 1986; Chylek, 2002) and variations in stream profile form (Rhea, 1993) are likely indicative of long-term Quaternary rock uplift. Debris flows generated from unchanneled valleys are often triggered by storm events and periodically scour steep, low-order channels. These debris flows are the primary erosional agent in the upper portions of the basins (Dietrich and Dunne, 1978; Stock and Dietrich, 2003), while in higher order channels fluvial incision into bedrock dominates.

Sediment yield measurements from undisturbed basins in the OCR range from 53 to 97 t km<sup>-2</sup> year<sup>-1</sup> (Brown and Krygier, 1971; Beschta, 1978). The average of these measurements is equivalent to a bedrock-lowering rate of 0.05 mm/year (Reneau and Dietrich, 1991). Reneau and Dietrich (1991) utilized dated deposits in hollows and calculated an average bedrock-lowering rate of 0.061 mm/year and an average exfoliation rate of 0.091 mm/year. An analy-

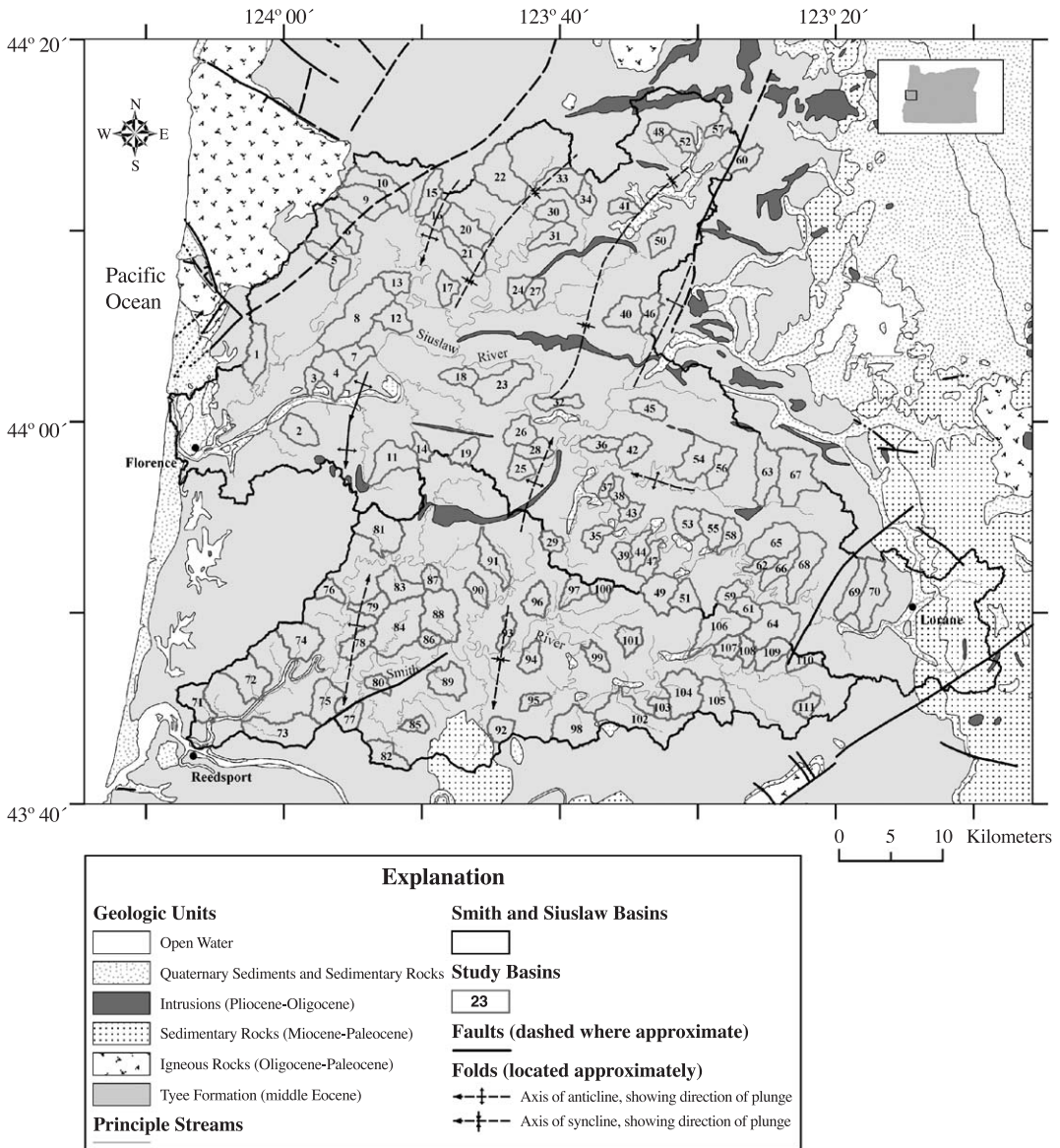


Fig. 1. Generalized geologic map of the Smith and Siuslaw Rivers area, showing locations of basins analyzed in this study (basin numbers keyed to Table 1). Geologic units and faults after the digitized version of Walker and MacLeod (1991). Folds located from Baldwin (1956).

sis of cosmogenic radionuclide accumulation in OCR soils yielded a catchment-averaged erosion rate of 0.12 mm/year (Heimsath et al., 2001). These diverse data sets span a range of spatial and temporal scales. The apparent agreement between sediment yield data and bedrock-lowering rates, in addition to the similarity of sediment yields in basins of varying sizes, has

been used to argue for an approximate erosional equilibrium in the OCR such that rates of denudation are spatially uniform (Reneau and Dietrich, 1991; Heimsath et al., 2001).

Variability in Holocene bedrock stream incision rates calculated from strath terraces, however, suggests that rates of denudation are variable in the OCR.

Specifically, relatively high incision rates ( $\sim 0.6\text{--}0.9$  mm/year) were found for the northern OCR and lower rates ( $\sim 0.1\text{--}0.3$  mm/year) in the central OCR with the transition occurring near  $44^{\circ}40'$  N (Personius, 1995). Stream incision data from the Smith and Siuslaw basins indicates a range of incision rates between 0 and 0.3 mm/year (Personius, 1995); however, the paucity of data points makes interpretation of local patterns tenuous. Personius (1993) documented anticlinal warping of Quaternary strath terraces along the Siuslaw River, apparently formed by the growth of a local fold. The variable Holocene incision rates and presence of deformed Quaternary features is inconsistent with the concept of erosional equilibrium as suggested by the sediment yield data. Further study is needed to look for any systematic patterns to the distribution of erosion rates in the OCR and to determine the sources of variability.

Because the Coast Range (i) has experienced rock uplift for several million years; (ii) remained unglaciated in the Pleistocene; and (iii) features relatively uniform lithology and precipitation rates over broad areas, the area appears ideally suited for using slope–area analysis to identify spatial variations in rock uplift. In our analysis, we focus on small basins ( $\sim 5\text{--}20$  km<sup>2</sup>) because uplift rates are likely to be less variable within each basin. Additionally, small basins are more likely to have adjusted their morphology to present climatic and uplift conditions (see Whipple, 2001, for a discussion of the time scale of response).

### 3. Slope–area analysis

Channel networks were extracted from 10-m digital elevation models (DEMs), and local channel slope ( $S$ ) and upstream drainage area ( $A$ ) were measured along the channel network. Considerable scatter is inherent in DEM-derived slope and area data (Snyder et al., 2000); thus, some smoothing of the data was required. Similar to other studies (Tarboton et al., 1991; Montgomery and Foufoula-Georgiou, 1993; Snyder et al., 2000), we averaged slopes in logarithmic bins of drainage area. Linear regression of the binned channel slope and upstream drainage area data allows direct measurement of  $k_s$  and  $\Theta$  as shown in Eq. (4).

The stream power incision model is only intended to represent fluvial incision into bedrock; thus, it is necessary to isolate the slope–area data associated with this process. A gradual change in the regression slope with decreasing area has been interpreted by many workers to correspond with the transition between debris flow-dominated and fluvial-dominated channel incision (Fig. 2) (Seidl and Dietrich, 1992; Moglen and Bras, 1995; Lague et al., 2003; Stock and Dietrich, 2003). This change in the power law scaling also appears to correspond to the location of preserved debris flow deposits in several study areas (Stock and Dietrich, 2003). Seidl and Dietrich (1992) found that this transition occurs between slopes of 0.2 and 0.3 in the OCR. Stock and Dietrich (2003) obtained a

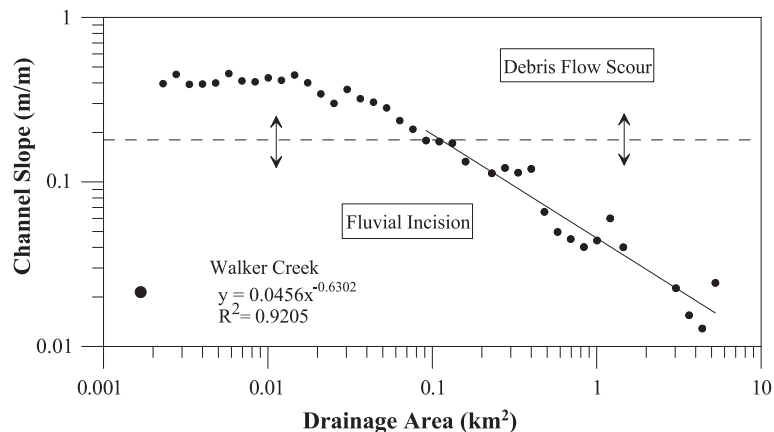


Fig. 2. Slope–area plot of Walker Creek basin (No. 7, Table 1) depicting process domains of debris flow scour and fluvial incision. Dashed line indicates the threshold slope value of 0.18 used in this study.

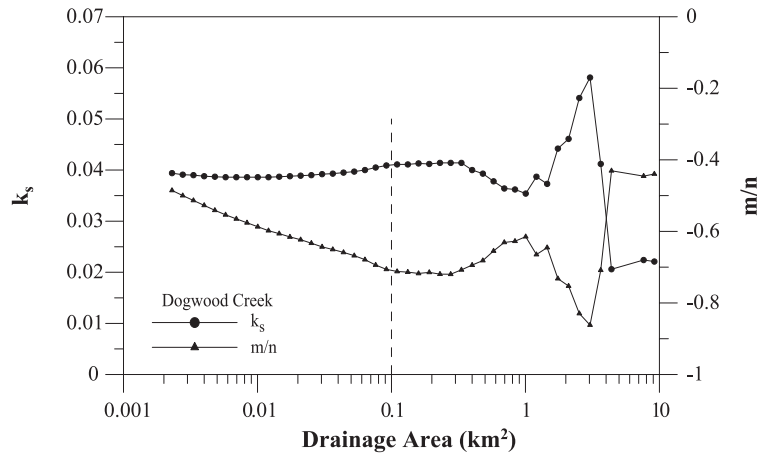


Fig. 3. Method to extract power law portion of the data applied to Dogwood Creek basin (No. 65, Table 1), showing variation in  $m/n$  ( $\blacktriangle$ ) and  $k_s$  ( $\bullet$ ) while larger drainage areas are successively pruned. Values converge around a drainage area of  $0.1 \text{ km}^2$  (dashed line).

more liberal estimate of the extent of debris flow influence and found the transition to fluvial processes to occur at slopes approximately equal to 0.1 in the OCR.

In order to determine the extent of the fluvial domain in our data sets, we used the method described by Stock and Dietrich (2003) of successively pruning the smallest drainage area data point and tracking both the slope and  $y$ -intercept of the resulting power law fits; the idea being that systematic changes in slope are indicative of data that

is not accurately described by a single power law. Fig. 3 indicates that the value of  $m/n$  stabilizes around a drainage area of  $0.1 \text{ km}^2$ . The value of  $k_s$  is strongly dependent on the value of  $m/n$ , and  $k_s$  also stabilizes at a drainage area of  $\sim 0.1 \text{ km}^2$ . Channel slopes at this particular drainage area are on the order of 0.11–0.26. In order to generate sufficient data and be conservative in our estimate of the fluvial domain, we used data with gradients  $< 0.18$  (Fig. 2). Although this approach may capture a portion of the channel network that

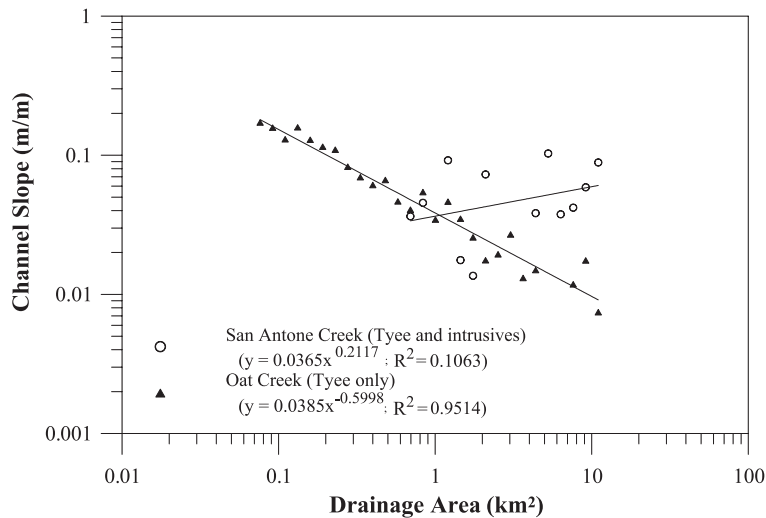


Fig. 4. Slope–area plot illustrating the effects of variable lithology on slope–area data: San Antone Creek (O). Slope–area data for a basin with uniform lithology is shown for comparison: Oat Creek (No. 54, Table 1,  $\blacktriangle$ ).

Table 1  
Slope–area statistics of basins analyzed in this study

Basin ID no.	Basin name <sup>a</sup>	Drainage area	$k_s$	$\Theta$	$R^2$
<i>Siuslaw Basins</i>					
1	UN NF Siuslaw River	9.01	0.041	0.54	0.77
2	Peterson Creek	7.45	0.028	1.03	0.92
3	Hanson Creek	3.07	0.047	0.74	0.82
4	David Creek	10.45	0.048	0.47	0.78
5	Porter Creek	8.41	0.030	0.86	0.89
6	Elma Creek	6.30	0.043	0.80	0.87
7	Walker Creek	5.71	0.046	0.63	0.92
8	McLeod Creek	23.30	0.041	0.70	0.93
9	Maria Creek	10.97	0.045	0.76	0.86
10	UN Indian Creek	10.46	0.039	0.72	0.91
11	UN Sweet Creek	11.01	0.022	0.75	0.96
12	Thompson Creek	7.00	0.064	0.57	0.65
13	Elk Creek	5.21	0.036	0.76	0.86
14	UN Hadsall Creek	3.28	0.070	0.67	0.76
15	Herman Creek	6.63	0.028	0.76	0.94
16	UN Taylor Creek	4.70	0.041	0.71	0.93
17	Velvet Creek	4.66	0.042	0.69	0.89
18	Brush Creek	5.08	0.074	0.54	0.77
19	UN Knowles Creek	5.00	0.068	0.61	0.91
20	UN Misery Creek	10.51	0.036	0.76	0.93
21	UN Deadwood Creek	8.22	0.070	0.66	0.90
22	UN Deadwood Creek	17.20	0.039	0.67	0.89
23	Barber Creek	12.50	0.055	0.56	0.93
24	Hollo Creek	4.91	0.068	0.61	0.76
25	UN Whittaker Creek	4.70	0.046	0.59	0.85
26	Waite Creek	6.82	0.051	0.56	0.82
27	Almasie Creek	3.91	0.045	0.55	0.86
28	Bounds Creek	5.38	0.048	0.66	0.89
29	UN Esmond Creek	3.42	0.036	0.72	0.93
30	UN Deadwood Creek	5.46	0.044	0.67	0.83
31	UN Bear Creek	7.03	0.065	0.70	0.90
32	Rock Creek	4.57	0.056	0.46	0.57
33	UN Deadwood Creek	8.22	0.077	0.86	0.79
34	UN Greenleaf Creek	4.30	0.070	0.36	0.65
35	Mill Creek	4.61	0.039	0.67	0.91
36	UN Siuslaw River	4.77	0.054	0.62	0.76
37	UN Fawn Creek	2.21	0.043	0.65	0.94
38	Pugh Creek	3.47	0.041	0.66	0.88
39	Haskins Creek	3.79	0.039	0.66	0.64
40	Knapp Creek	8.67	0.040	0.61	0.93
41	Pontius Creek	3.68	0.032	1.07	0.95
42	Saleratus Creek	6.82	0.061	0.77	0.91
43	North Creek	3.22	0.038	0.68	0.88
44	Clay Creek	5.22	0.047	0.55	0.79
45	Cattle Creek	5.34	0.066	0.54	0.82
46	Haynes Creek	5.87	0.046	0.64	0.91
47	Bierce Creek	4.61	0.044	0.73	0.85
48	UN Lake Creek	3.47	0.080	0.81	0.77
49	Oxbow Creek	9.53	0.043	0.62	0.88
50	UN Fish Creek	4.85	0.068	0.65	0.84
51	Bear Creek	6.04	0.035	0.69	0.88

Table 1 (continued)

Basin ID no.	Basin name <sup>a</sup>	Drainage area	$k_s$	$\Theta$	$R^2$
<i>Siuslaw Basins</i>					
52	UN Lake Creek	3.70	0.065	0.72	0.89
53	Layne Creek	6.83	0.046	0.70	0.77
54	Oat Creek	11.60	0.039	0.60	0.95
55	Camp Creek	6.36	0.036	0.81	0.90
56	Grenshaw Creek	6.78	0.034	0.67	0.84
57	UN Lake Creek	3.30	0.048	0.90	0.88
58	Conger Creek	4.78	0.036	0.68	0.88
59	Doe Hollow Creek	4.87	0.041	0.61	0.74
60	UN Swartz Creek	6.95	0.069	0.45	0.75
61	Fryingpan Creek	4.78	0.042	0.56	0.80
62	Holland Creek	3.12	0.038	0.59	0.77
63	Swamp Creek	10.47	0.031	0.61	0.94
64	Buck Creek	14.70	0.038	0.69	0.91
65	Dogwood Creek	12.50	0.041	0.71	0.96
66	Bottle Creek	5.83	0.042	0.69	0.75
67	UN Panther Creek	16.10	0.026	0.59	0.92
68	Doe Creek	12.70	0.045	0.70	0.94
69	Fawn Creek	8.42	0.043	0.65	0.94
70	Douglas Creek	12.50	0.036	0.69	0.93
Mean			0.047	0.67	0.85
<i>Smith Basins</i>					
71	UN Smith River	8.48	0.017	0.81	0.94
72	Joyce Creek	12.20	0.047	0.57	0.83
73	Otter Creek	16.13	0.028	0.90	0.83
74	Eslick Creek	11.50	0.056	0.53	0.89
75	Murphy Creek	9.41	0.051	0.70	0.90
76	Sulpher Creek	4.15	0.061	0.55	0.77
77	Perkins Creek	5.01	0.071	0.42	0.62
78	Railroad Creek	6.62	0.065	0.70	0.93
79	Georgia Creek	5.21	0.064	0.53	0.75
80	Taylor Creek	3.16	0.067	0.67	0.94
81	UN NF Smith River	14.32	0.062	0.59	0.95
82	UN Wasson Creek	7.02	0.080	0.49	0.78
83	Cedar Creek	9.02	0.057	0.61	0.96
84	Spencer Creek	20.11	0.058	0.63	0.92
85	UN Wasson Creek	3.01	0.065	0.60	0.65
86	UN Bear Creek	2.87	0.067	0.52	0.75
87	UN MF Smith River	3.86	0.046	0.62	0.90
88	UN Johnson Creek	14.89	0.047	0.68	0.86
89	Buck Creek	9.02	0.063	0.88	0.89
90	UN WF Smith River	4.45	0.037	0.73	0.96
91	Beaver Creek	7.86	0.034	0.64	0.91
92	UN Vincent Creek	4.99	0.052	0.78	0.94
93	Coldwater Creek	3.52	0.051	0.58	0.88
94	UN Beaver Creek	4.87	0.055	0.55	0.87
95	UN Big Creek	3.21	0.055	0.73	0.96
96	UN North Sister Creek	6.20	0.048	0.57	0.94
97	UN North Sister Creek	5.25	0.042	0.68	0.82
98	Mosetown Creek	13.15	0.047	0.75	0.92
99	Devils Club Creek	4.16	0.053	0.66	0.92
100	UN North Sister Creek	3.56	0.042	0.64	0.78

Table 1 (continued)

Basin ID no.	Basin name <sup>a</sup>	Drainage area	$k_s$	$\Theta$	$R^2$
<i>Smith Basins</i>					
101	UN South Sister Creek	4.94	0.048	0.72	0.95
102	Halfway Creek	19.97	0.044	0.63	0.86
103	Johnson Creek	3.41	0.052	0.64	0.90
104	Cleghorn Creek	13.21	0.048	0.64	0.92
105	Little South Fork	11.03	0.037	0.74	0.93
106	Panther Creek	13.77	0.033	0.68	0.93
107	Salmonberry Creek	4.36	0.030	0.61	0.72
108	Elk Creek	3.80	0.029	0.60	0.78
109	Beaver Creek	6.60	0.034	0.64	0.91
110	Summit Creek	4.62	0.031	0.61	0.81
111	Sleezer Creek	3.73	0.038	0.68	0.79
Mean			0.049	0.65	0.86

<sup>a</sup> UN refers to unnamed channels which are tributary to the channel whose name follows.

experiences debris flow deposition (Stock and Dietrich, 2003), our goal here is not to differentiate zones of process dominance but instead systematically document variation in channel gradient across our study area.

Because we use relatively small basins in this study and a significant portion of the drainage basins are debris flow-dominated, the data used in our analysis represent a relatively small portion of the total channel length in each individual catchment. By this approach, we are attempting to strike a balance between the quantity of slope–area data used in each study basin and the spatial resolution of variation in  $k_s$ . The analysis of small basins enables us to better characterize spatial variations in channel gradient across the central OCR. Based on our results, data with slopes < 0.18 tend to be well represented by a power law function and do not show significant curvature that would affect the power law exponent (Fig. 2). Importantly, the choice of a particular threshold slope does not have a significant influence on our results, as over the range of published debris flow–fluvial transition slopes in the OCR from 0.3 to 0.04, recalculated values of  $k_s$  vary by < 15%.

Comparison of steepness index ( $k_s$ ) values between drainage basins is complicated by the inherent dependence of the regression intercept on the regression slope (Sklar and Dietrich, 1998; Kirby et al., 2003). Normalizing drainage area by a representative drain-

age area ( $A_r$ ) in the center of the range of data reduces the dependence of  $k_s$  on the ratio  $m/n$ . Rewriting Eq. (4) yields a nondimensional coefficient (Sklar and Dietrich, 1998):

$$S = S_r(A/A_r)^{-m/n} \tag{7}$$

where  $S_r$  is a representative slope, and

$$S_r = S(A_r) = k_s A_r^{-m/n} \tag{8}$$

Because the slope threshold is typically encountered at a drainage area of around 0.1 km<sup>2</sup> and we analyzed basins on the order of 10.0 km<sup>2</sup>, we chose  $A_r$  as to occupy the approximate middle of our data sets such that  $k_s$  is the average channel slope at a drainage area of 1.0 km<sup>2</sup>.

To explore spatial patterns in bedrock channel form, we calculated an interpolated grid of our estimates of  $k_s$ . Whereas the analysis of a single channel profile within a large catchment tends to smooth out variations in channel slope, our approach enables us to evaluate variability in  $k_s$  and explore potential correlations with geologic structure. Importantly, in this contribution, we did not attempt to test the conceptual framework of Eq. (1); instead, we used it as a guide for identifying potential variations in the rate of tectonic forcing.

In addition to mapping the distribution of channel gradients across our study area, we applied the stream power model (Eq. (4)) to estimate how variability in  $k_s$  values may translate into differences in the rate of rock uplift. For this endeavor, we invoke the steady-state assumption for our local basins, such that bedrock gradients adjust rapidly to variations in rock uplift rate. To assess the magnitude of differential uplift from measurements of  $k_s$ , we can use Eq. (6) evaluated for two distinct drainage basins and calculate the ratio of  $k_s$  (subscripts 1 and 2):

$$k_{s1}/k_{s2} = (U_1/K_1)^{1/n1} / (U_2/K_2)^{1/n2} \tag{9}$$

Assuming  $K$  and  $n$  are constant between basins (which is well supported in our study area):

$$K_1 = K_2 \tag{10}$$

and

$$n_1 = n_2 \quad (11)$$

Eq. (9) reduces to:

$$U_1/U_2 = (k_{s1}/k_{s2})^n \quad (12)$$

By solving Eq. (12) using previously calibrated estimates of  $n$ , we can use the ratio  $k_{s1}/k_{s2}$  to estimate the magnitude of the differential uplift represented by the pattern of  $k_s$ .

#### 4. Results

We calculated slope–area data for 111 basins with uniform lithology in the  $\sim 2900\text{-km}^2$  area of the Smith and Siuslaw watersheds, resulting in an average point density of  $0.038$  points/ $\text{km}^2$ . To explore how nonuniform lithology affects channel steepness, we also calculated slope–area data for several basins containing both Tye Formation and intrusive igneous rocks. These multilithology data sets are not described well by a single power law (calculated values of  $r^2$  were consistently less than  $0.4$ ) and thus lead to highly variable values of the concavity index and the steepness index. In some

cases, variable lithology leads to slope–area plots depicting convex-up basins such as San Antone Creek (Fig. 4). In the absence of local-scale geologic maps, such a pattern could be interpreted as evidence for systematically varying rock uplift rate ( $\odot$  in Fig. 4). In contrast, basins that have only Tye Formation as bedrock are universally concave up and well described by a single power law (e.g., Fig. 4, Oat Creek).

Values of  $k_s$  for the basins with uniform Tye lithology ranged from  $0.017$  to  $0.08$  (Table 1). The  $k_s$  values have a roughly normal distribution (Fig. 5), and the variation by a factor of  $\sim 4$  reflects heterogeneity with respect to bedrock channel slopes. Such variability is not consistent with spatially uniform rates of erosion and rock uplift. Example slope–area plots for basins with high and low values of  $k_s$  in both the Smith and Siuslaw watersheds are shown in Fig. 6. Values of  $\Theta$  for basins comprised only of Tye Formation range from  $0.36$  to  $1.07$  (Table 1) but are generally clustered between  $0.5$  and  $0.8$  with a mean value of  $0.66$  (Fig. 7). This result is consistent with reported values from other studies (Howard and Kerby, 1983; Whipple and Tucker, 1999; Snyder et al., 2000; Kirby and Whipple, 2001; Kirby et al., 2003). Although we observed a weakly defined correlation between  $\Theta$  and  $k_s$  consistent with other

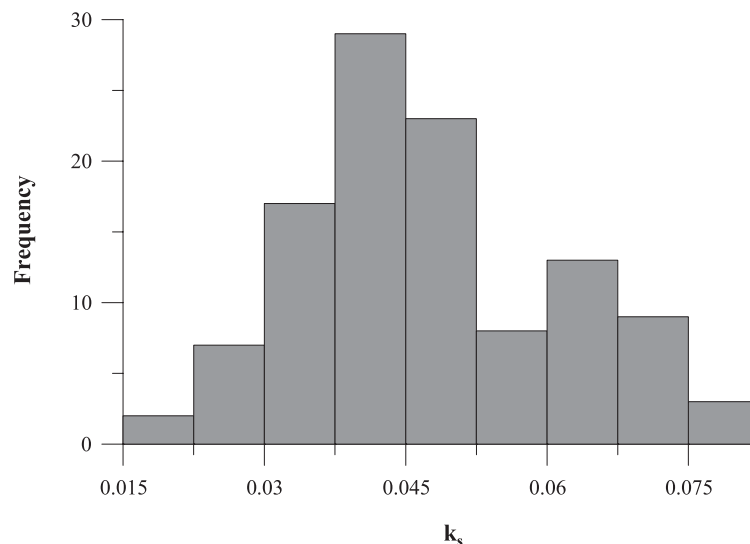


Fig. 5. Histogram of the steepness index ( $k_s$ ) for Smith and Siuslaw tributary basins with uniform lithology.

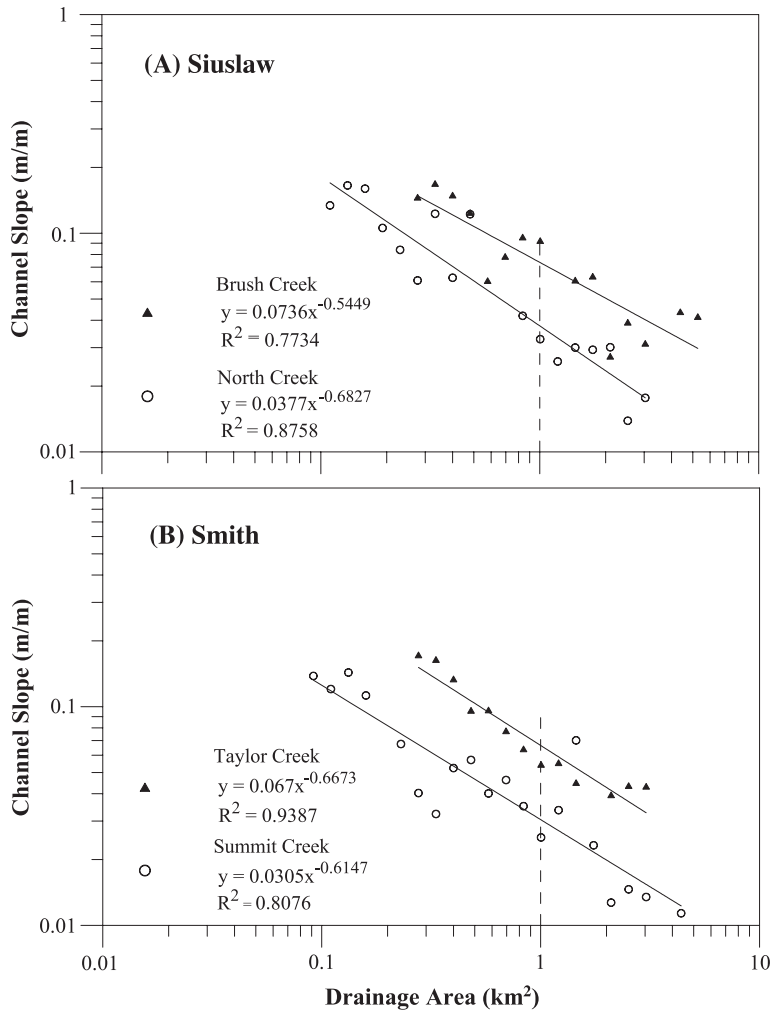


Fig. 6. Example slope–area plots for basins showing both high and low  $k_s$  values. (A) Siuslaw tributary basins: Brush Creek (No. 18, Table 1, ▲), North Creek (No. 43, ○). (B) Smith tributary basins: Taylor Creek (No. 80, ▲), Summit Creek (No. 110, ○). Dashed line indicates the drainage area value of 1 km<sup>2</sup> where  $k_s$  is calculated.

studies (e.g., Sklar and Dietrich, 1998), the magnitude of covariation is small relative to observed spatial variability in  $k_s$ .

Our contoured map of  $k_s$  (Fig. 8) reveals a systematic pattern to the distribution of  $k_s$  throughout the study area. Values are low ( $\sim 0.35$ ) in the NW and SE portions of the study area, and an  $\sim 20$ -km-wide belt of elevated values ( $\sim 0.65$ ) trending NE by SW runs through the central portion of the study area. The orientation of this zone appears to follow the trend of weakly defined folds in the Tyee Formation, although the wavelength of

the observed  $k_s$  variation is much greater than that suggested by individual folds. Some of the folds follow the pattern closely (e.g., westernmost anticline in Smith Basin), but others show no obvious correlation (e.g., westernmost anticline in Siuslaw Basin). Due to dense vegetation and infrequent exposure, limited bedrock attitudes, and low dip angles, structural relationships are difficult to constrain (Baldwin, 1956); however, some of the folds appear to be better defined than others, perhaps explaining this discrepancy. Most generally, our results show a consistent band of channel slopes

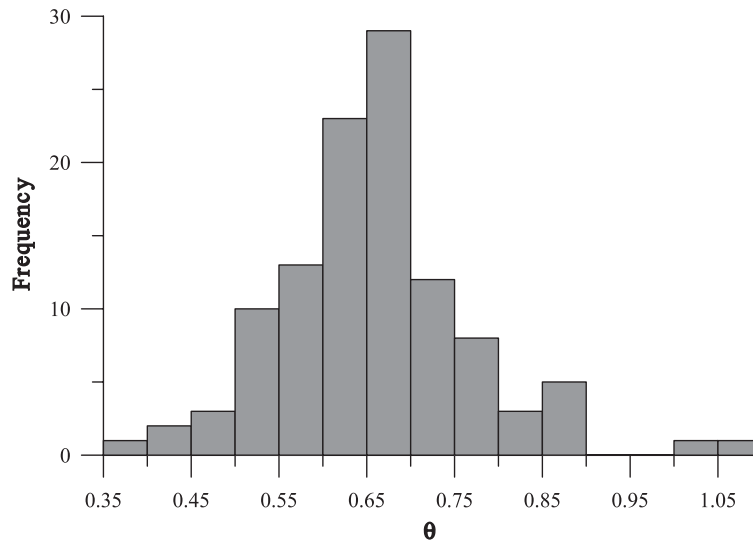


Fig. 7. Histogram of the concavity index ( $\theta$ ) for Smith and Siuslaw tributary basins with uniform lithology.

that are twice as steep as catchments to the east and west (Fig. 8).

In order to investigate the relationship of this pattern to mapped structures, we generated two cross-sections along the central axis of the Smith and Siuslaw watersheds, roughly perpendicular to the strikes of folds (see Fig. 8). The resulting cross-sections demonstrate systematic E–W oriented variation in  $k_s$  (Fig. 9). Fig. 9 (A–A') shows low values of  $k_s$  in the western and eastern portions of the Siuslaw basin and a region of elevated values centered near km 20. Neither of the two anticlines appear to be coincident with local maxima of  $k_s$ , instead they appear to bound the region of high  $k_s$ , such that large gradients in  $k_s$  occur across the folded region. Fig. 9 (B–B') reveals a broad pattern of increasing  $k_s$  to the east, with a maxima near km 15, and decreasing values farther east. The anticline appears to be roughly coincident with maximum  $k_s$  values; however, the fold spacing is inconsistent with the observed variation in  $k_s$ . These rough correlations suggest that the distribution of  $k_s$  may be related to differential uplift associated with the growth of local folds.

Although a physical explanation of controls on the value of  $n$  in Eq. (4) has yet to be demonstrated, we used our results to estimate the magnitude of differential uplift across the central OCR. Using a range of published estimates of  $n$  from 0.66 to 1.0

and Eq. (12), we calculated that rates of rock uplift in our study area may vary by a factor of 3–4. We compared the average value of  $k_s$  in the broad swath of elevated values ( $k_s$  equal to 0.065) to average coastal and inland estimates ( $k_s$  equal to 0.035). This calculation suggests that the area represented by the belt of elevated channel slopes (see reddish colors in Fig. 8) may be experiencing rock uplift rates 1.5–1.9 times greater than in the coastal and inland areas.

## 5. Discussion

Values of the steepness index are variable across the studied portion of the central OCR and exhibit low values in the SE and NW portions of the study area with a N–S-trending belt of elevated values through the central portion. Many factors may play a role in generating this pattern including orographic precipitation gradients, lithologic variations, a transient response to tectonic or climatic pulses, and long-term differential uplift rates.

### 5.1. Orographic precipitation

Variations in orographic precipitation have been shown to influence the curvature of steady-state river

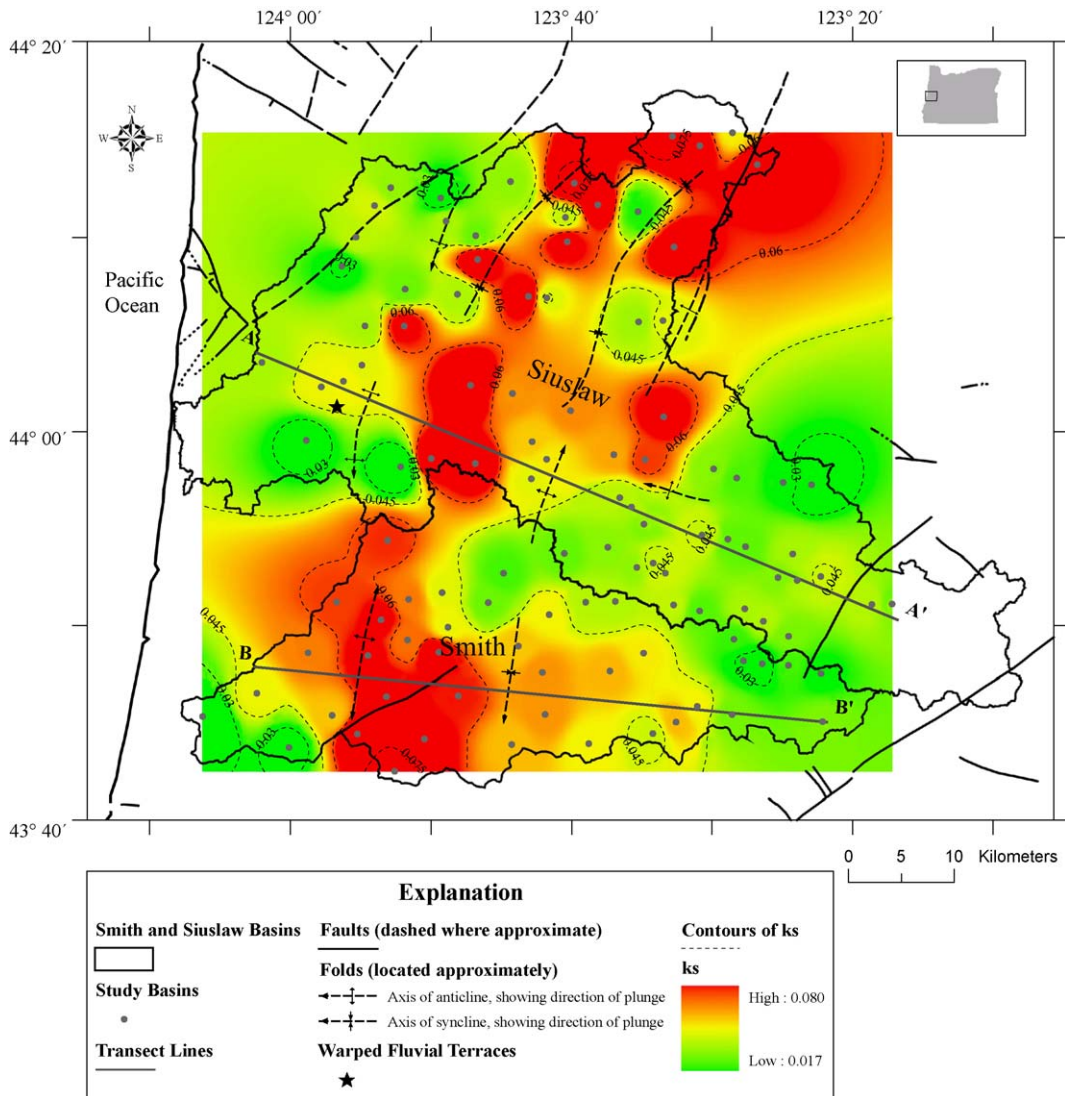


Fig. 8. Contour map of  $k_s$ . Faults after the digitized version of Walker and MacLeod (1991). Folds located from Baldwin (1956). Star indicates the location of warped fluvial terraces (Personius, 1993). A–A' and B–B' indicate the locations of cross sections plotted in Fig. 9.

profiles (Roe et al., 2002). This could complicate analysis of river profile response to spatially variable uplift rates. Annual precipitation rates from stations at the coast, in the central portion of the range, and on the western side of the Willamette Valley (Reedsport, Noti, and Fern Ridge Dam) are 190, 160, and 100 cm/year, respectively (NOAA, 1999). Thus, precipitation varies across the study area by less than a factor of 2, and rates are generally highest at the coast and decrease inland. This pattern is inconsistent with our findings that  $k_s$  is

low in the western and eastern portions of the study area and elevated in the middle. Thus, our results are not consistent with variable precipitation generating the observed pattern of channel steepness.

### 5.2. Lithology

Variations in erosivity due to lithologic variations can have a major influence on the value of  $K$  in the stream power incision model. Although all of the

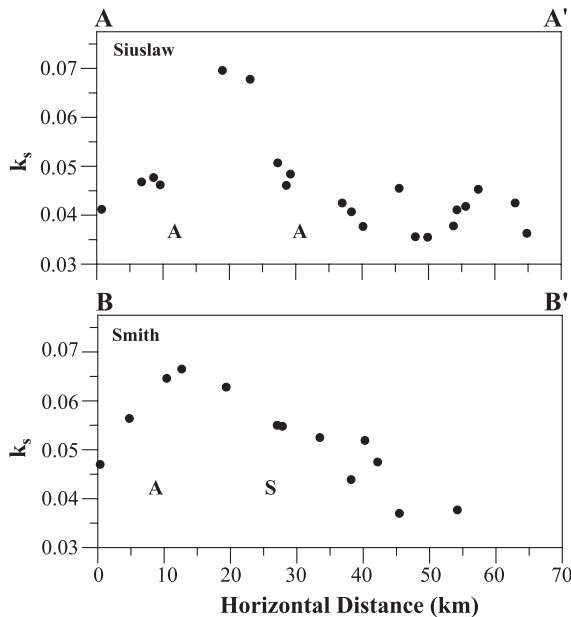


Fig. 9. Transects of  $k_s$  oriented perpendicular to the strike of mapped folds (transect locations shown on Fig. 8). A–A': Siuslaw River, B–B': Smith River. A and S refer to the approximate location of anticlines and synclines respectively.

study basins analyzed here are exclusively Tye Formation, some heterogeneity in the form of variable sandstone/siltstone ratios is present within the Tye. Due to the depositional setting of the forearc basin (which has been rotated clockwise over  $60^\circ$  since the middle Eocene), these differences are most pronounced in a N–S orientation (Chan and Dott, 1983; Heller and Ryberg, 1983; Heller and Dickinson, 1985), which is contrary to the predominantly E–W variations in channel steepness observed here. Rock mass strength estimates at various locations within the Smith and Siuslaw basins reveal a narrow range of values (Personius, 1995). Thus, lithologic variation is unlikely to generate the observed pattern of channel morphology.

### 5.3. Transient response/base level fall

Climatically or tectonically induced changes in base level may be introduced as discrete pulses near the coast that propagate up the river network as the system adjusts to changes in the rate of base-level lowering. In response to sea-level fluctuation and rock uplift, the

Siuslaw and Smith rivers may transmit pulses of locally accelerated incision upstream in the form of knick-points. If such transient pulses contributed to the pattern of  $k_s$  values observed here, we might expect to see a correlation between  $k_s$  and along-channel distance from the coast. Our data do not show such a correlation; instead, we see elevated values at various locations within each watershed. The consistency of  $k_s$  values across the drainage divide between the Smith and Siuslaw basins also seems contradictory to the notion of a transient phase in base-level lowering, as we might expect the two basins to respond independently.

### 5.4. Sediment flux

Variations in profile gradient may be driven by fluctuations in sediment flux as the relative abundance of sediment to abrade the bed should affect incision rate (Sklar and Dietrich, 2001). In contrast to other field settings, the configuration of hillslopes and debris flow source areas is similar across the OCR. We do not see evidence for systematic variations in sediment supply across the drainage basins in our study area. Additionally, our analysis is focused on basins of similar size and  $k_s$  does not vary systematically with drainage area; thus, variations in sediment flux due to variations in drainage area may be minimal. Nonetheless, the influence of sediment supply and grain size on bedrock channel incision could introduce complex feedbacks modulating topographic development; such analyses are beyond the scope of this contribution.

### 5.5. Differential rock uplift

The overall pattern of  $k_s$  throughout the study area may be reflective of differential cumulative uplift of the central OCR. Estimates of stream incision rates from uplifted fluvial terraces in the Siuslaw and Smith watersheds range from 0.0 to 0.3 mm/year (Personius, 1995), and estimates of bedrock-lowering rates from dated colluvial deposits range from 0.031 to 0.112 mm/year (Reneau and Dietrich, 1991). The magnitudes of these variations are consistent with our findings that uplift rates vary by a factor of 2–4 in these watersheds; however, the pattern of the variation is difficult to compare to the pattern of  $k_s$  (Fig. 8), owing to the sparsity of available denudation data at the local scale. Although our data do not extend to the coast, all of the

westernmost basins in our study area indicate consistently low values of  $k_s$ . This result is consistent with the findings of Kelsey et al. (1996) that uplift rates for the past  $\sim 125$  ka along the coast in this portion of the OCR are relatively constant and  $\sim 0.1$  mm year<sup>-1</sup>.

Mitchell et al. (1994) found that geodetic uplift rates along a profile extending east from Reedsport varied from  $\sim 2$  mm/year at the coast to approximately zero in the eastern OCR. The magnitude of this variation is consistent with our findings that uplift rates vary longitudinally across the study area by a factor of 2–4. The pattern of geodetic uplift rates is quite different from the pattern of  $k_s$ , however. While geodetic rates are highest along the coast and decrease inland, our pattern suggests long-term uplift rates are highest in the central portion of the range and decrease both inland and toward the coast. Geodetic uplift rates probably record elastic strain accumulation during interseismic periods between subduction events (Weldon, 1991; Mitchell et al., 1994). Because geodetic rates constitute only a portion of the seismic cycle and may not reflect the long-term pattern of rock uplift, comparison of geodetic and long-term uplift rates is difficult.

The origin of variability in  $k_s$  is difficult to constrain. One possible interpretation for the pattern is the seaward migration of a deformation front that currently produces rapid ( $\sim 4$  mm/year) interseismic uplift rates along the coast of central Oregon. If the pattern of  $k_s$  is instead related to the growth of local structures, their spatial pattern is more easily explained, as geodetic uplift rates are interpreted to represent subduction-related deformation, not local structural control. The correspondence of mapped structures to the location of large gradients in  $k_s$  supports this interpretation. This hypothesis is complicated, however, by the necessity of accommodating significant shortening associated with these structures. Folds in the Tyee Formation exhibit very low amplitudes on the order of 1 km over 20 km (and thus are difficult to define based on limited structural data) such that long-lived strain along these structures would have resulted in greater shortening than observed. Strictly interpreted, this indicates that folding of the Tyee Formation may be more recent (Plio-Pleistocene) such that zones of higher uplift are manifested in channel morphology. This hypothesis is supported by the presence of multiple fluvial terraces displaying anticlinal warping near Mapleton (see Fig. 8). The age of these surfaces is inferred to be on the

order of 100 ka (Personius, 1993), consistent with recent shortening. The uniformity of  $k_s$  values to the east and west of the N–S band of steepened channels supports the interpretation of local structures causing rock uplift rates to exceed background values.

### 5.6. Implications for debris flow frequency

Our results have profound implications for debris flow potential in the central OCR. Elevated channel gradients in the fluvial portion of basins should translate to steeper unchanneled valleys at the upper extent of the channel network (Stock and Dietrich, 2003). These concave regions accumulate thick ( $\sim 1$ –3 m) soil mantles via transport from surrounding hillslopes and are preferential source areas for shallow landslides that often transform into debris flows (Dietrich and Dunne, 1978; Montgomery and Dietrich, 1994; Dietrich et al., 1995). The cyclic evacuation and infilling of topographic hollows controls sediment production in the OCR (Benda, 1990; Benda and Dunne, 1997). Simple analyses of slope stability indicate that all else equal, thinner soils are required to generate failure in steeper unchanneled valleys (Dietrich et al., 1995). Thus, steeper source areas should experience more frequent shallow landsliding and be more sensitive to factors that affect slope stability such as reduction of root strength due to fire or land management (Schmidt et al., 2001). Quantitative estimates of how landslide frequency may vary for given changes in hollow slope require analysis of soil transport rates and hillslope morphology (Roering et al., 1999). Based on field and air photo-based observations from recent storms (1964, 1996, and 2001), watersheds proximal to Mapleton, OR (which is located within the band of elevated channel slopes) have experienced significant shallow landslide activity (Swanston and Swanson, 1976; Robison et al., 1999). Evaluation of debris flow potential in the OCR may benefit from consideration of broad patterns of channel network steepness as presented here.

## 6. Conclusions

Slope–area analysis of 111 small drainage basins indicates that bedrock channel slopes vary systemat-

ically, and by a factor of  $\sim 4$  across the central OCR. In particular, the spatial distribution of the steepness index indicates low values in the NW and SE portions of the study area and a N–S-trending belt of elevated values running through the central portion of the study area. Although many factors may have influenced this pattern, orographic effects, lithologic variations, variations in sediment flux, and transient climatic or tectonically induced pulses are unlikely candidates. These findings suggest that rates of rock uplift and erosion may not be spatially constant throughout the central OCR, but instead vary systematically.

Differential rock uplift of the central OCR seems the most plausible explanation for the distribution of channel slopes, and through the use of the stream power incision model we find that the uplift rates may vary by a factor of  $\sim 2$  across the study area. These variations may result from the growth of local folds or from cumulative differential uplift related to subduction processes. The magnitude of variation is consistent with variations found in both stream incision rate estimates and in geodetic uplift data. The apparent correspondence of mapped structures to large gradients in  $k_s$  supports the hypothesis of local structural control; however, the necessity of accommodating significant shortening with low-amplitude folds remains problematic. The correspondence of watersheds experiencing frequent shallow landslides during historical storms with the region of elevated channel slopes suggests that the region of elevated channel steepness may be highly sensitive to land use practices and high-intensity rainstorms.

### Acknowledgements

Discussions and excursions with Rebecca Dorsey and Sarah Chylek were most helpful in formulating the project goals, and the authors wish to acknowledge Siobhan McConnell for assistance in editing the manuscript.

### References

- Ahnert, F., 1970. Functional relationships between denudation relief and uplift in large, mid-latitude drainage basins. *American Journal of Science* 268 (3), 243–263.
- Baldwin, E.M., 1956. Geologic map of the Lower Siuslaw River Area, Oregon. Oil and Gas Investigations Map 01-0186, Reston, VA.
- Baldwin, E.M., 1986. *Geology of Oregon*, 3rd ed. Kendall/Hunt Publishing, Dubuque, IA. 170 pp.
- Benda, L.E., 1990. The influence of debris flows on channels and valley floors in the Oregon coast range, USA. *Earth Surface Processes* 15, 457–466.
- Benda, L., Dunne, T., 1997. Stochastic forcing of sediment supply to channel networks from landsliding and debris flows. *Water Resources Research* 33, 2849–2863.
- Beschta, R.L., 1978. Long-term patterns of sediment production following road construction and logging in the Oregon coast range. *Water Resources Research* 14, 1011–1016.
- Brown, G.W., Krygier, J.T., 1971. Clear-cut logging and sediment production in the Oregon coast range. *Water Resources Research* 7, 1189–1198.
- Chan, M.A., Dott, R.H., 1983. Shelf and deep-sea sedimentation in Eocene forearc basin, western Oregon; fan or non-fan? *American Association of Petroleum Geologists* 67 (11), 2100–2116.
- Chylek, S.J., 2002. GIS analysis of Quaternary stream capture in the eastern Coast Range, western Oregon. BS Thesis, University of Oregon, Eugene. 55 pp.
- Dietrich, W.E., Dunne, T., 1978. Sediment budget for a small catchment in mountainous terrain. *Zeitschrift für Geomorphologie* 29, 191–206.
- Dietrich, W.E., Reiss, R., Hsu, M.-L., Montgomery, D.R., 1995. A process-based model for colluvial soil depth and shallow landsliding using digital elevation data. *Hydrological Processes* 9, 383–400.
- Dietrich, W.E., Bellugi, D., Sklar, L.S., Stock, J.D., Heimsath, A.M., Roering, J.J., 2003. Geomorphic transport laws for predicting landscape form and dynamics. In: Iverson, R.M., Wilcock, P. (Eds.), *Prediction in Geomorphology*. American Geophysical Union, Washington, DC, pp. 103–132.
- Finlayson, D.P., Montgomery, D.R., Hallet, B., 2002. Spatial coincidence of rapid inferred erosion with young metamorphic massifs in the Himalayas. *Geology* 30 (3), 219–222.
- Granger, D.E., Kirchner, J.W., Finkel, R., 1996. Spatially averaged long-term erosion rates measured from in situ-produced cosmogenic nuclides in alluvial sediments. *Journal of Geology* 104 (3), 249–257.
- Hancock, G.S., Anderson, R.S., Whipple, K.X., 1998. Beyond power: bedrock river incision process and form. In: Tinkler, K., Wohl, E.E. (Eds.), *Rivers over Rock: Fluvial Processes in Bedrock Channels*. Geophysical Monograph Series, vol. 107. American Geophysical Union, Washington, DC, pp. 35–60.
- Heimsath, A.M., Dietrich, W.E., Nishiizumi, K., Finkel, R.C., 2001. Stochastic processes of soil production and transport: erosion rates, topographic variation and cosmogenic nuclides in the Oregon coast range. *Earth Surface Processes and Landforms* 26, 531–552.
- Heller, P.L., Dickinson, W.R., 1985. Submarine ramp facies model for delta-fed, sand-rich turbidite systems. *American Association of Petroleum Geologists Bulletin* 69 (6), 960–976.

- Heller, P.L., Ryberg, P.T., 1983. Sedimentary record of subduction to forearc transition in the rotated Eocene basin of western Oregon. *Geology* 11 (7), 380–383.
- Howard, A.D., 1994. A detachment-limited model of drainage basin evolution. *Water Resources Research* 30, 2261–2285.
- Howard, A.D., Kerby, G., 1983. Channel changes in badlands. *Geological Society of America Bulletin* 94, 739–752.
- Howard, A.D., Seidl, M.A., Dietrich, W.E., 1994. Modeling fluvial erosion on regional to continental scales. *Journal of Geophysical Research* 99, 13971–13986.
- Hurtrez, J.-E., Lucazeau, F., 1999. Lithologic control on relief and hypsometry in the Hérault drainage basin (France). *Comptes Rendus de l'Académie des Sciences. Series IIA, Sciences de la terre et des planètes* 328 (10), 687–694 (*Earth and Planetary Science*).
- Kelsey, H.M., 1990. Late quaternary deformation of marine terraces on the Cascadia subduction zone near Cape Blanco, Oregon. *Tectonics* 9, 983–1014.
- Kelsey, H.M., Bockheim, J.G., 1994. Coastal landscape evolution as a function of eustasy and surface uplift rate, Cascadia margin, southern Oregon. *Geological Society of America Bulletin* 106, 840–854.
- Kelsey, H.M., Engebretson, D.C., Mitchell, C.E., Ticknor, R., 1994. Topographic form of the Coast Ranges of the Cascadia margin in relation to coastal uplift rates and plate subduction. *Journal of Geophysical Research* 99, 12245–12255.
- Kelsey, H.M., Ticknor, R.L., Bockheim, J.G., Mitchell, C.E., 1996. Quaternary upper plate deformation in coastal Oregon. *Geological Society of America Bulletin* 108 (7), 843–860.
- Kirby, E., Whipple, K., 2001. Quantifying differential rock-uplift rates via stream profile analysis. *Geology* 29 (5), 415–418.
- Kirby, E., Whipple, K.X., Tang, W., Chen, Z., 2003. Distribution of active rock uplift along the eastern margin of the Tibetan Plateau: inferences from bedrock channel longitudinal profiles. *Journal of Geophysical Research* 108 (B4), 2217 (10.1029/2001JB000861).
- Lague, D., Crave, A., Davy, P., 2003. Laboratory experiments simulating the geomorphic response to tectonic uplift. *Journal of Geophysical Research-Solid Earth* 108 (B1), 2008 (10.1029/2002JB001785).
- McNeill, L.C., Goldfinger, C., Kulm, L.D., Yeats, R.S., 2000. Tectonics of the Neogene Cascadia forearc basin: investigations of a deformed late Miocene unconformity. *Geological Society of America Bulletin* 112 (8), 1209–1224.
- Mitchell, C.E., Vincent, P., Weldon II, R.J., Richards, M.A., 1994. Present-day vertical deformation of the Cascadia margin, Pacific Northwest, United States. *Journal of Geophysical Research* 99 (B6), 12257–12277.
- Moglen, G.E., Bras, R.L., 1995. The effect of spatial heterogeneities on geomorphic expression in a model of basin evolution. *Water Resources Research* 31, 2613–2623.
- Montgomery, D.R., 2001. Slope distributions, threshold hillslopes, and steady-state topography. *American Journal of Science* 301 (4–5), 432–454.
- Montgomery, D.R., Brandon, M.T., 2002. Topographic controls on erosion rates in tectonically-active mountain ranges. *Earth and Planetary Science Letters* 201 (3–4), 481–489.
- Montgomery, D.R., Dietrich, W.E., 1994. A physically based model for the topographic control on shallow landsliding. *Water Resources Research* 30 (4), 1153–1171.
- Montgomery, D.R., Foufoula-Georgiou, E., 1993. Channel network source representation using digital elevation models. *Water Resources Research* 29, 1178–1191.
- Montgomery, D.R., Schmidt, K.M., Greenberg, H.M., Dietrich, W.E., 2000. Forest clearing and regional landsliding. *Geology* 28 (4), 311–314.
- National Oceanic and Atmospheric Administration (NOAA), 1999. United States monthly precipitation data (<http://lwf.ncdc.noaa.gov/oa/climate/online/coop-precip.html>).
- Neim, W.A., 1976. Drainage basin morphology in the central Coast Range, Oregon. MS Thesis, Oregon State University, Corvallis. 100 pp.
- Ohmori, H., 1993. Changes in the hypsometric curve through mountain building resulting from concurrent tectonics and denudation. *Geomorphology* 8 (4), 263–277.
- Personius, S.F., 1993. Age and origin of fluvial terraces in the central Coast Range, western Oregon. U.S. Geological Survey Bulletin 2038. 56 pp.
- Personius, S.F., 1995. Late Quaternary stream incision and uplift in the forearc of the Cascadia subduction zone, western Oregon. *Journal of Geophysical Research* 100 (B10), 20193–20210.
- Reneau, S.L., Dietrich, W.E., 1991. Erosion rates in the southern Oregon Coast Range: evidence for an equilibrium between hillslope erosion and sediment yield. *Earth Surface Processes and Landforms* 16, 307–322.
- Rhea, S., 1993. Geomorphic observations of rivers in the Oregon Coast Range from a regional reconnaissance perspective. *Geomorphology* 6, 135–150.
- Robison, E.G., Mills, K., Paul, J., Dent, L., Skaugset, A., 1999. Storm Impacts and Landslides of 1996: Final Report. Oregon Dept. of Forestry, Salem, OR.
- Roe, G.H., Montgomery, D.R., Hallet, B., 2002. Effects of orographic precipitation variations on the concavity of steady-state river profiles. *Geology* 30 (2), 143–146.
- Roe, G.H., Montgomery, D.R., Hallet, B., 2003. Orographic precipitation and the relief of mountain ranges. *Journal of Geophysical Research* 108 (6), 2315 (10.1029/2001JB001521).
- Roering, J.J., Kirchner, J.W., Dietrich, W.E., 1999. Evidence for nonlinear, diffusive sediment transport on hillslopes and implications for landscape morphology. *Water Resources Research* 35 (3), 853–870.
- Schmidt, K.M., Roering, J.J., Stock, J.D., Dietrich, W.E., Montgomery, D.R., Schaub, T., 2001. The variability of root cohesion as an influence on shallow landslide susceptibility in the Oregon coast range. *Canadian Geotechnical Journal* 38 (5), 995–1024.
- Schorghofer, N., Rothman, D.H., 2001. Basins of attraction on random topography. *Physical Review. E, Statistical Physics, Plasmas, Fluids, and Related Interdisciplinary Topics* 63, 6302.
- Seidl, M.A., Dietrich, W.E., 1992. The problem of channel erosion into bedrock. In: Schmidt, K.H., DePloey, J. (Eds.), *Functional Geomorphology*. Catena. Supplement, vol. 23. Catena-Verlag, Cremlingen, Germany, pp. 101–124.
- Sklar, L., Dietrich, W.E., 1998. River longitudinal profiles and

- bedrock incision models: stream power and the influence of sediment supply. *Geophysical Monograph* 107, 237–260.
- Sklar, L.S., Dietrich, W.E., 2001. Sediment and rock strength controls on river incision into bedrock. *Geology* 29 (12), 1087–1090.
- Snively, P.D., 1987. Tertiary geologic framework, neotectonics, and petroleum potential of the Oregon–Washington continental margin. In: Scholl, D.W., Grant, A., Vedder, J.G. (Eds.), *Geology and Resource Potential of the Continental Margin of Western North America and Adjacent Ocean Basins: Beaufort Sea to Baja California*. Earth Science Series, vol. 6. Circum-Pacific Council for Energy and Mineral Resources, Houston, TX, pp. 305–335.
- Snyder, N.P., Whipple, K.X., Tucker, G.E., Merritts, D.J., 2000. Landscape response to tectonic forcing: digital elevation model analysis of stream profiles in the Mendocino triple junction region, northern California. *Geological Society of America Bulletin* 112 (8), 1250–1263.
- Stock, J., Dietrich, W.E., 2003. Valley incision by debris flows: evidence of a topographic signature. *Water Resources Research* 39 (4), 1089 (10.1029/2001WR001057).
- Stock, J.D., Montgomery, D.R., 1999. Geologic constraints on bedrock river incision using the stream power law. *Journal of Geophysical Research* 104 (B3), 4983–4993.
- Swanston, D.N., Swanson, F.J., 1976. Timber harvesting, mass erosion, and steep-land forest geomorphology in the Pacific Northwest. In: Coates, D.R. (Ed.), *Geomorphology and Engineering*. Dowden, Hutchinson & Ross, Stroudsburg, PA, pp. 199–221.
- Tarboton, D.G., Bras, R.L., Rodriguez-Itrube, I., 1991. On the extraction of channel networks from digital elevation data. *Hydrological Processes* 5, 81–100.
- van der Beek, P., Bishop, P., 2003. Cenozoic river profile development in the upper Lachlan catchment (SE Australia) as a test of quantitative fluvial incision models. *Journal of Geophysical Research* 108 (6), 2309 (10.1029/2002JB002125).
- Walker, G.W., Duncan, R.A., 1989. *Geologic Map of the Salem 1 degrees by 2 degrees Quadrangle, Western Oregon*. Miscellaneous Investigations Series-U.S. Geological Survey, vol. I-1893. Reston, VA.
- Walker, G.W., MacLeod, N.S., 1991. *Geologic map of Oregon*. Special map U.S. Geological Survey, Reston, VA.
- Weldon II, R.J., 1991. Active tectonic studies in the United States, 1987–1990. U.S. National Report to the International Union of Geodesy and Geophysics. *Reviews of Geophysics*, vol. 29, pp. 890–906.
- Wells, F.G., Peck, D.L., 1961. *Geologic Map of Oregon West of the 121st Meridian*. Miscellaneous Investigations Series-U.S. Geological Survey, vol. I-325. Reston, VA.
- West, D.O., McCrumb, D.R., 1988. Coastline uplift in Oregon and Washington and the nature of Cascadia subduction-zone tectonics. *Geology* 16, 169–172.
- Whipple, K.X., 2001. Fluvial landscape response time: how plausible is steady-state denudation? *American Journal of Science* 301, 313–325.
- Whipple, K.X., Tucker, G.E., 1999. Dynamics of the stream-power river incision model: implications for the height limits of mountain ranges, landscape response timescales, and research needs. *Journal of Geophysical Research* 104 (B8), 17661–17674.
- Whipple, K.X., Hancock, G.S., Anderson, R.S., 2000. River incision into bedrock: mechanics and relative efficacy of plucking, abrasion, and cavitation. *Geological Society of America Bulletin* 112, 490–503.